Electron Tagger for H1 Experiment at HERA2

V.Andreev[1], P.Baranov[1], A.Belousov[1], V.Boudry[2], A.Fomenko[1], L.Gorbov[1], I.Herynek[3], J.Hladky[3], A.Lebedev[1], I.Lebedev[1], E.Malinovsky[1], F.Moreau[2], S.Rusakov[1], I.Sheviakov[1], L.Shtarkov[1], P.Smirnov[1], Yu.Soloviev[1], A.Specka[2], A.Usik[1], Y.Vazdik[1]

[1] *Lebedev Physical Institute, 119991 Moscow, Russia*
[2] *LPNHE, Ecole Polytechnique, IN2P3-CNRS, 91128 Palaiseau, France*
[3] *Institute of Physics,18040 Praha, Czech Republic*

July 17, 2002

Abstract

Description of the new electron detector (tagger ET6) for the H1 luminosity monitor at upgraded *ep* collider HERA2 is given. The detector is used for tagging photoproduction events and for a cross check of the luminosity measurements. It is placed at the distance approximately 6 m from *ep* interaction point, inside the quadrupole of modified HERA magnet system. The tagger consists of a compact scintillation fiber calorimeter (Spacal) developed in two options on the basis of tungsten or lead passive material. Both versions of calorimeter were studied in electron test beams at DESY and CERN at energies E=1.6–27.6 GeV. The energy and space resolutions were measured and found to be $\sigma_E/E = (18.6/\sqrt{E} \oplus 3.2)\%$, $\sigma_x = (4.3/\sqrt{E} \oplus 0.6)\ mm$, $\sigma_y = (5.9/\sqrt{E} \oplus 0.3)\ mm$ for tungsten detector and $\sigma_E/E = (13.0/\sqrt{E})\%$, $\sigma_x = \sigma_y = (7.2/\sqrt{E})\ mm$ for lead detector (E is in GeV). The energy resolutions are in reasonable agreement with MC calculations.

1 Introduction

The ep collider HERA provided wide the program of investigations in the interactions of 27.5 GeV electrons with 920 GeV protons at the designed luminosity $1.5 \cdot 10^{31}\ cm^{-2}s^{-1}$. The HERA upgrade 2000 [1] to achieve $\approx$ 5-fold increase in the ep-collision luminosity will open new perspectives for a deeper insight in the matter structure at extremely short distances.

The increase in the luminosity will be attained by magnetic compression of beams in the interaction point (IP) that demands the essential modification of the HERA beam optics in the vicinity of $\pm 40\ m$ around IP. This leads to the necessity to change completely all configuration of the existing electron taggers of the H1 luminosity monitor. In particular the old tagger ET33 [2] which was placed at the distance 33 m from IP downstream electron beam has been replaced with a new tagger.

The most important demand for the new tagger is be ability to detect the recoil electrons at forward angles in the process

$$e + p \longrightarrow e' + X \tag{1}$$

mediated by exchange of almost real photons ($Q^2 \leq 0.01 GeV^2/c^2$) in order to study the soft and hard photoproduction reactions at c.m. energies which are inaccessible for fixed target accelerators.

The new tagger design meets the problems which are connected with the very tight geometry in the vicinity of the collider IP. The MC calculations of recoil electron trajectories (see Fig.1) using the package [3] at the specific choice of vacuum tract for the upgraded HERA (HERA2) show that new tagger has to be placed at the distance $\approx 6\ m$ from the IP between the poles of quadrupole GI1. The height and width of the tagger is limited by the magnet gap size and should not exceed 27x90 mm^2.

MC simulation of hadron production events in the process (1)

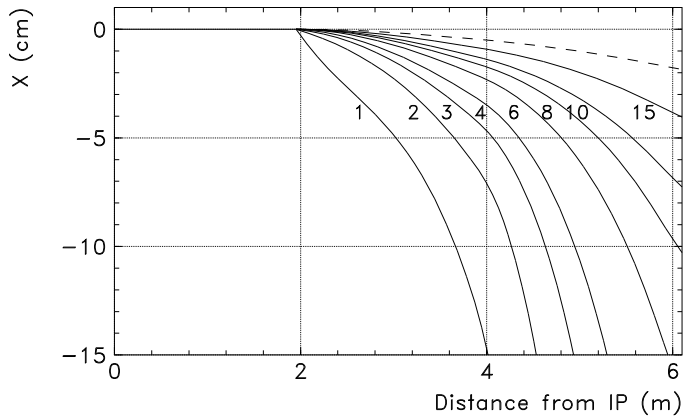

Fig. 1: The trajectories of recoil electrons with energies from 1 GeV to 27.5 GeV downstream the IP (dashed curve corresponds to 27.5 GeV).

shows (see scatter plot Fig.2a) that recoil electrons stay within the vertical strip of $Y_{e'} = \pm\ 1.5\ cm$ relative the e beam axis for ET6 position near the beam pipe of 4 cm radius. Its optimal lateral width is determined by the $x_{e'} - E_{e'}$ correlation plot (Fig.2b) as $\approx 8\ cm$. The special beam pipe with exit window of 75.4 mm width for the recoil electrons was manufactured. This width corresponds (as the MC simulation of the energy distribution of detected electrons, Fig.2c, and ET6 acceptance, Fig.2d show) to the energies E of recoil electron in the range 6–15 GeV. This is enable the study of photoproduction processes at γ-p c.m. energies $\sqrt{s} = (215 - 270)\ GeV$. Thus the new tagger (ET6) provides conditions for the study of photon induced reactions in approximately the same energy range as the old ET33.

The new tagger is (as ET33 was) simultaneously used for the cross check of the HERA luminosity measurements and for the electron/photon mutual energy calibration using BH bremsstrahlung process

$$e + p \longrightarrow e' + \gamma + p \tag{2}$$

and the specific requirements of this process to the new tagger are close to those from (1).

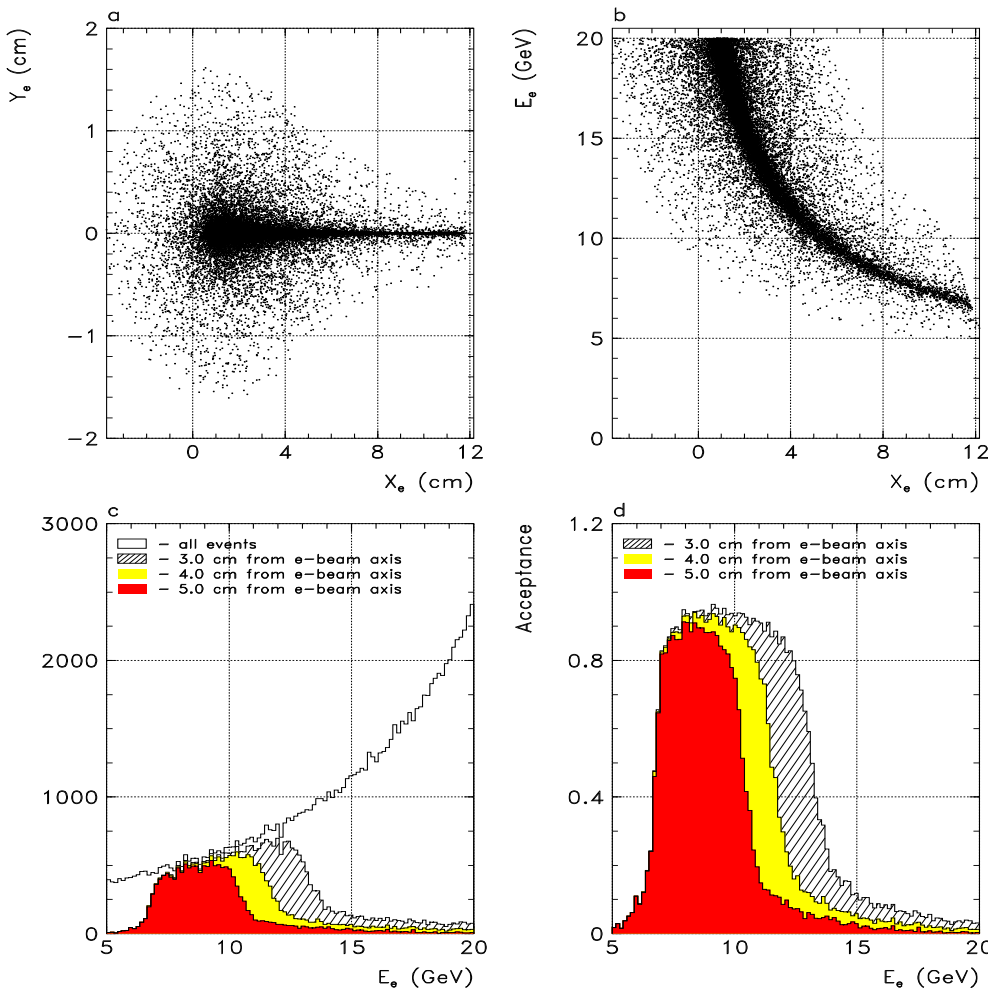

Fig. 2: Scatter plot (a), correlation plot (b), events *vs* energy distribution of electrons (c) and acceptance (d) for ET6 .

According to demands of processes (1) and (2) the tagger should have parameters: (a) the energy resolution better than $25\%/\sqrt{E[GeV]}$, (b) the linearity of detector response at the level 1%, (c) the space resolution $\sim 2\,mm$ for the H1 energies, (d) small transverse sizes. In order to satisfy these requirements compact, small size SPACAL type calorimeters (tungsten-fiber and lead-fiber) were manufactured for ET6 with 6x2 cells granulation in accordance with the proposal [4].

The construction of taggers is described in Section 2. Section 3 contains the results of the ET6 detector studies in the DESY electron test beam at energies 1.6-6 GeV. The results of CERN tests for energies 6-27.6 GeV are given in the Section 4. Summary and conclusion are in the last Section.

2 Calorimeter design

The ET6 calorimeter contains scintillating fibers of 0.5 mm diameter embedded in the tungsten or lead block. Charge particles of an electromagnetic shower produced by final state electrons e' of processes (1) and (2) in tungsten (W) or lead (Pb) material evoke in scintillating fibers the light which is detected by photomultipliers (PM) which are placed in the iron box to be shielded from scattered magnetic fields. Two types of PM were checked in the readout during tests – Philips XP1911 and FEU-147. The study of BICRON BCF-12 fibers at LPI electron synchrotron at Troitsk [5] revealed their low radiation resistivity; therefore KURARAY SCSN81 fibers of refraction index 1.59 were opted for ET6. The good radiation hardness of chosen fiber material [6] allows to sustain the tagger6 irradiation by recoil electrons from bremsstrahlung process (2) – the annual absorbed dose does not exceed 20 $kRad$ for integrated luminosity 200 pb^{-1} per year expected at HERA2.

The tungsten calorimeter of ET6 (Fig.3) consists of 2 blocks of size 35x24x130 mm. Each block has 33x22 holes of 0.6 mm diameter where scintillating fibers are placed. Vertical raws of holes are shifted

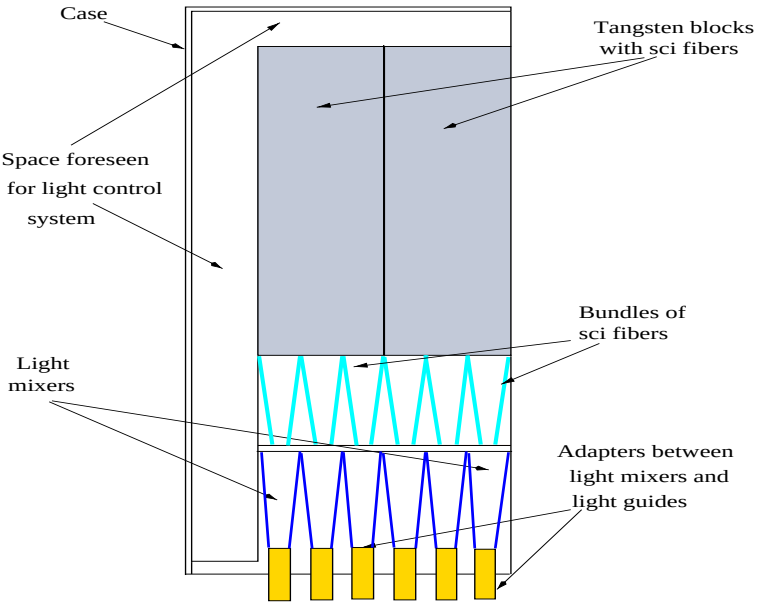

Fig. 3: The schematic view of tungsten ET6.

relative to neighbouring ones in chess order. The fibers to W volume ratio is 1:4.45 and tungsten density is 17 g/cm^3. The corresponding radiation length and Moliere radius are equal to $X_0 = 4.05\ mm$ and $R_m = 10.2\ mm$. So the length of the calorimeter is $\approx 32 \cdot X_0$. One W block has 6 cells (3x2 matrix) containing 11x11 fibers each. The cell size is $\approx$11.7x12 mm^2. The fibers of a cell are gathered in circular bundle of $\approx$ 6 mm diameter at the back side (relative to the e-beam direction) of the calorimeter and glued by blackened epoxy. The edges of bundles are cut off by the sharp chisel after the epoxy became hard. The light transportation to PM is performed by clear light guides preceded by light mixers. The front edge of the calorimeter was covered by mirrored mylar to reflect scintillation light back to fibers and thus to improve the light collection.

The light mixers have a cut square pyramid shape. They are made of high transparent Polystyrene (PS) of the same refraction index as fibers and attached to bundles so that square light mixer surface covers completely the bundle circle. The mixer length is 32.5 mm. Its fiber bundle side and light guide side have sizes 7.9x7.9 mm^2 and 5.1x5.1 mm^2 respectively. The light mixers are placed in the aluminum housing which has screw connectors for light guides attachment. The light guides are assembled of approximately ninety 0.5 mm diameter KURARAY Clear-PS fibers which are placed in plastic tube and glued at both ends to 5.6 mm diameter circle bundles. They have the length $\approx$ 50 cm and deliver scintillation light to PMs Philips XP1911 or FEU-147 with the cathode diameter of 15 mm and 10 mm respectively. Two W blocks are attached to each other by 0.1 mm nonmagnetic metal band and placed into the 101x246x26 mm^3 case made of 0.5 mm thickness stainless steel.

The lead calorimeter of ET6 has 12 cells (6x2 matrix). It is assembled of 30 Pb plates of the size 0.78x75.6x200 mm^3 with 84 grooves on one side where scintillating fibers are placed. The plates were prepared of spare parts of H1 SPACAL electromagnetic calorimeter

[7, 8]. The active to passive material volume ratio for this calorimeter is 1:2.26 and the values $X_0 = 9\ mm$ and $R_m = 25.4\ mm$ are approximately twice larger than for the tungsten case. But the length in X_0 is smaller: $\approx 22 \cdot X_0$. The groves of subsequent horizontal layers are shifted to provide more uniform sampling. The light collection system is similar to W case with the difference that the number of scintillating fibers in one cell is greater (210 instead of 121) and the fibers are gathered to the square bundle of the size 7.5x7.5 mm^2. The light mixers have the bigger foot (9x9 mm^2) to cover the larger bundle and they are longer (38.3 mm). So the length of the housing is larger than for the tungsten detector. One cell contains 14x15 fibers and has the size $\approx$ 12.6x11.7 mm^2. Thin strip of white Teflon is attached to the front end of the calorimeter to serve for better light collection. Lead plates are coupled by the band of 0.1 mm thickness

Table 1: Main parameters of two spacal detectors.

Parameter	unit	Tungsten	Lead
Absorber Density	$[g/cm^3]$	17.0	11.3
Fibers (Scint.)		Kuraray SCSN81	Kuraray SCSN81
Cell X x Y x Z	$[mm^3]$	11.7 x 12.0 x 130	12.6 x 11.7 x 200
Fiber/Hole Diam.	$[mm]$	0.5 / 0.6	0.5 / 0.5
Num.fibers/Cell		11 x 11 = 121	14 x 15 = 210
Act. : Pass. (vol)		1 : 4.45	1 : 2.26
Rad.Length X_o	$[mm]$	4.05	9.0
Moliere radius R_m	$[mm]$	10.2	25.4
Matrix of Cells		6 x 2	6 x 2
HalfX x HalfY	$[R_m^2]$	3.44 x 1.18	1.49 x 0.46
Full length	$[X_o]$	32	22

stainless steel and placed into the box of size 25x105x317 mm^3 made of 0.3 mm thickness steel. The steel is nonmagnetic.

The main parameters of detectors are summarized in the Table 1.

3 Tungsten and lead calorimeters study at DESY

The calorimeters were investigated at the DESY electron test beam 21. The beam is provided by DESY2 synchrotron where electrons accelerated to energy 7 GeV hit internal 10 μm diameter carbon fiber target to produce the bremsstrahlung photons. Then these photons are converted to e^+e^--pairs in Cu target of 3 mm thick. The electrons passing through collimators and 2 bending magnets reach the test beam hall. By the choice of magnetic field electrons of definite energy in the interval 1–6 GeV are selected. The Fig.4 gives

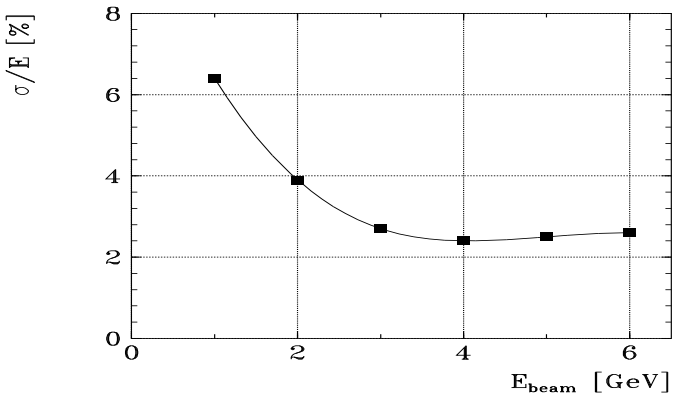

Fig. 4: Energy spread of DESY test beam (MC simulation).

the MC prediction for the energy spread of beams.

The layout of the test beam facility is shown in Fig.5. The studi-

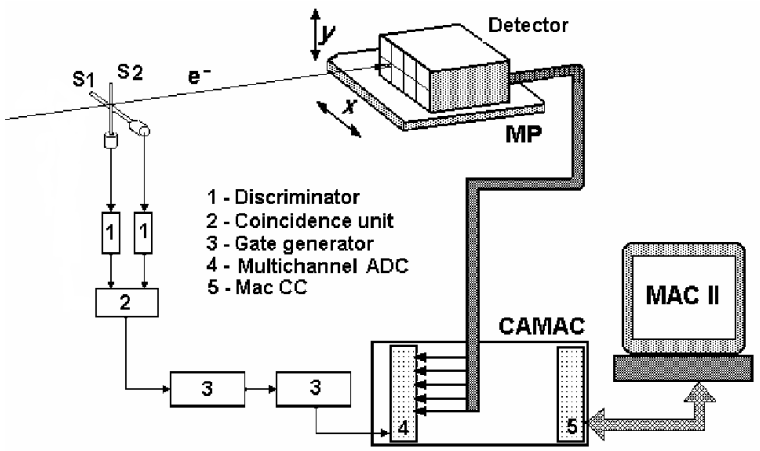

Fig. 5: Test-beam scheme.

ed detector was placed on the movable platform (MP) to provide

the space scan in horizontal (x) and vertical (y) directions with the precision $\approx 0.2\ mm$. The trigger was generated by coincidence of scintillation counters S1 and S2 that restricts beam spot to the size 3x3 mm^2.

CAEN HV system SY127 was used to supply PMs FEU-147 and XP1911. Signals from PMs were digitized by LeCroy CAMAC Model 2249A 12 channel charge ADC with 10 bits resolution. 100 ns duration gate was produced by NIM gate generator LeCroy model 222.

3.1 Linearity of response and energy resolution

The signals from different channels have to be equalized. Therefore the calorimeter has been scanned in the beam horizontally and vertically with energy of 3 GeV and the beam spot was centered at each of the cells. The cells responses have been equalized roughly within 10% by tuning high voltage on PM. Only 4 adjoined cells (2x2 matrix) of the calorimeter were chosen for the study at DESY tests. Relative calibration coefficients have been found after pedestal subtraction and the amplitude spectra have been fitted by for several energies in the interval 1.6-6 GeV and entry point of the beam in the area 2x2 mm^2 around the center of each cell. The energy scan was performed with the beam spot in the center of (2x2) matrix to measure linearity and resolution of energy response. Final calibration coefficients have been obtained by normalization of relative calibration coefficients to the sum of amplitudes of all channels fitted by Gaussian.

The energy response for both (W and Pb) calorimeters shows the linear dependence (better than 1%) on e-beam energy (Fig.6) which is found to be independent of PM type.

Fig.7 displays energy dependence of σ_E/E for W and Pb calorimeters obtained using photomultipliers FEU-147 and Philips XP1911. The beam energy spread (Fig.4) was included into experimental er-

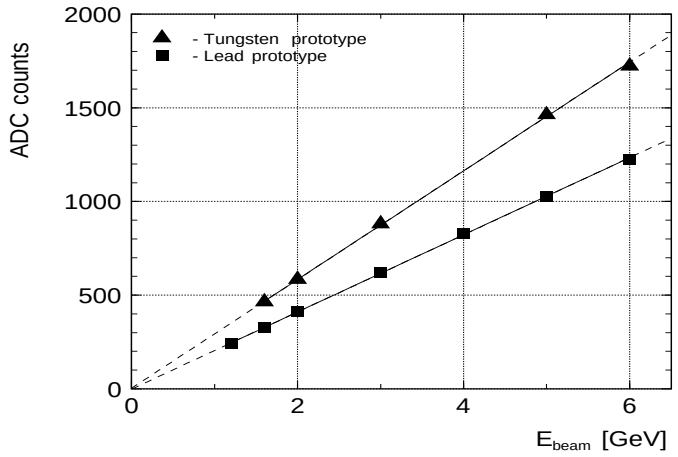

Fig. 6: The energy dependence of mean amplitude (sum of 4 ADC counts).

rors. The MC predictions for energy resolution are also on the pictures for comparison.

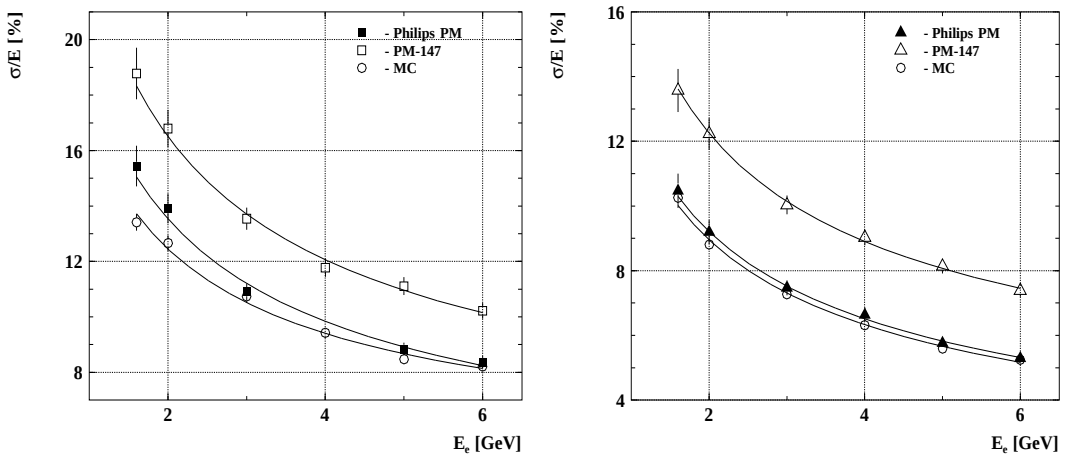

Fig. 7: The energy resolution *vs* electron energies for W (left) and Pb (right) detectors.

The experimental data and the results of MC simulations were fitted by the quadratic sum of a stochastic and constant terms:

$$\frac{\sigma_E}{E} = \frac{a}{\sqrt{E}} \oplus b \tag{3}$$

The results of fitting for different experiments are given in Table 2. The solid curves in the Fig.7 present the relevant fits.

One can see that the best energy resolution is achieved in the lead calorimeter and the MC supports this finding. This result is connected with smaller volume ratio of passive to active material in

lead calorimeter in comparison with tungsten one. It is also seen that the use of PM Philips XP1911 leads to better energy resolution and thus is more preferable.

It should be stressed that the measured σ_E/E exceeds the MC prediction especially for the FEU-147 application. This may be connected with the PM photostatistic influence which was not taken into account in the simulation. The corresponding contribution to σ_E/E for PM of photon detector of upgraded luminosity monitor [4] can reach several per cents [9].

Table 2: Fits of energy resolution by $\sigma_E/E = a/\sqrt{E[GeV]} \oplus b$.

data source	Detector	PM	$a(\%)$	$b(\%)$	χ^2/N
DESY data	W	Philips	18.6±0.8	3.2±1.0	2.0/5
DESY data	Pb	Philips	13.0±1.0	0.0±1.0	0.2/6
DESY data	W	FEU-147	22.5±1.0	4.3±1.2	1.6/6
DESY data	Pb	FEU-147	16.8±0.6	2.9±0.9	0.2/6
MonteCarlo	W	not.inkl.	16.3±0.4	4.7±0.4	3.7/6
MonteCarlo	Pb	not.incl.	12.6±0.40	0.3±1.2	1.6/6

3.2 Data for shower profile and MC for space resolution

To estimate the space resolution σ_x (which also influences on the accuracy of energy reconstruction) the x-scan of both detectors was performed along the horizontal border of upper and lower raws of cells. The ratio of the ADC signals sum for pair of vertical cells (A_1) to the sum for adjacent vertical pair (A_2) (shower profile) is shown in the Fig.8 as a function of the distance x counted from the vertical boundary between cells (x=0).

The shower profile for lead calorimeter was obtained from the DESY test data at e-beam energy 3 GeV. For the tungsten case

the CERN data at the energy 15 GeV are displayed in the figure (see also the next section).

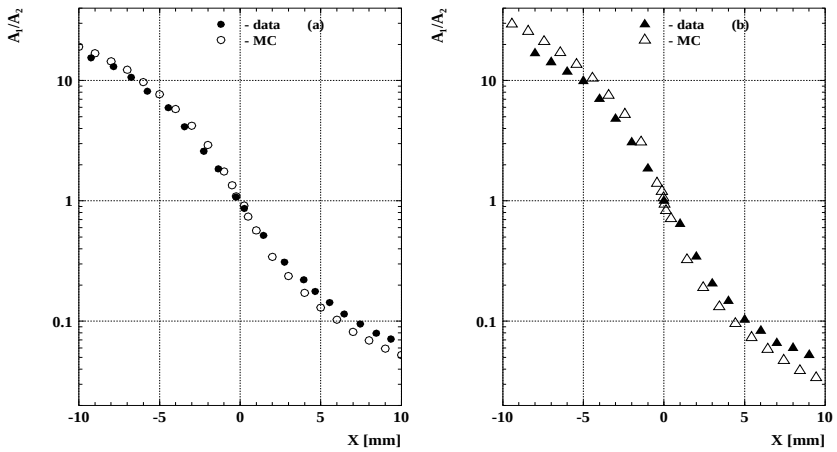

Fig. 8: The shower profile for (a) Pb, E=3 GeV, and (b) W, E=15 GeV, calorimeters.

It is seen that the ratio A_1/A_2 is rather sensitive to the x-position of electron hit point especially near the border of adjacent cells. MC simulation closely follows the experimental data near this border but deviates from data at far end of the cells especially for W calorimeter.

There is no tracking device at the DESY test beam to determine the e-hit point coordinate with a good precision. With the 3 mm lateral size of the beam it is only possible to estimate roughly the space resolution of detectors. Therefore the MC simulation is used to obtain σ_x.

In the MC the structure of (3x2) cells was considered (Fig.9). The real sizes of W and Pb calorimeter cells were used in the simulation

1	2	3
4	5	6

Fig. 9: (3x2) matrix of calorimeter cells considered in MC simulation.

which was carried out for the energy E=6 GeV. The hit points are spread in rectangular region 0.5(vert.)x12(horiz.) mm^2 along the

horizontal border of cells 2 and 5 with the zero point in the center of (3x2) matrix.

The reconstruction of hit points was performed using shower profile function for each of two pairs of cells one of which is always the cell with maximum energy deposit and two others are adjacent cells, with subsequent energy weighting of the two obtained coordinates.

The correlation plots between initial hit point x_{beam} and reconstructed coordinate x_{rec} are shown in Fig.10 for both detectors. One

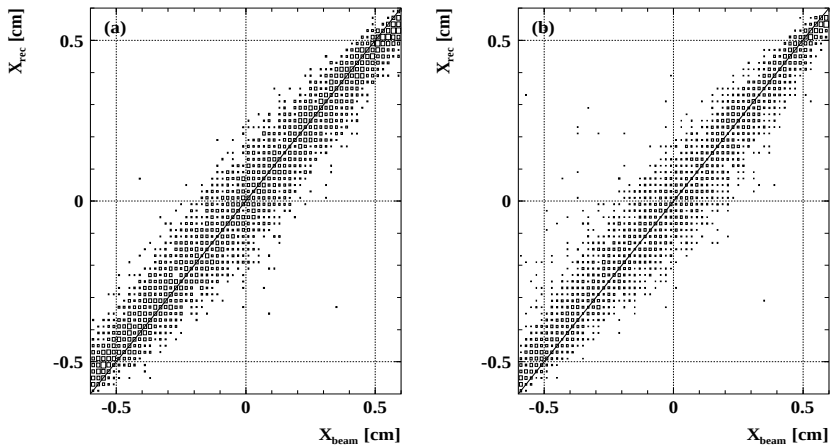

Fig. 10: MC for correlation between x_{beam} and x_{rec} at E=6 GeV for Pb (a) and W (b) calorimeters.

can see that the reconstruction procedure for MC events works quite well – the correlation is evident.

The distributions of the difference between reconstructed coordinate and initial hit point obtained in MC is given in the Fig.11. Gaussian fit of these distributions shows that accuracy of space reconstruction at E=6 GeV averaged over the area of central cells (2 and 5) is

$$\sigma_x = (0.74 \pm 0.01)\ mm \quad for\ lead\ calorimeter \tag{4}$$

and

$$\sigma_x = (0.65 \pm 0.01)\ mm \quad for\ tungsten\ calorimeter \tag{5}$$

Thus MC shows that tungsten detector can provide better space resolution than the lead one but the difference is not big. It should

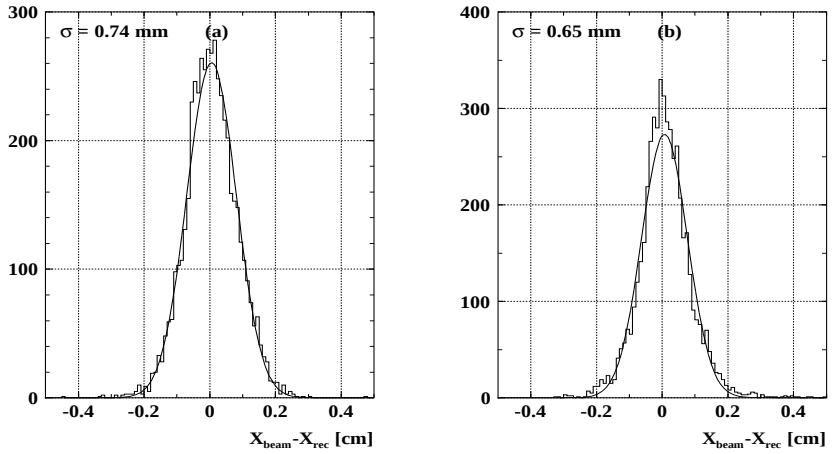

Fig. 11: The MC prediction for distribution of the difference $x_{beam} - x_{rec}$ for Pb (a) and W (b) calorimeters at E=6 GeV.

be mentioned that in the measurements with the real detector these values will be larger. The shown errors are due to the statistics only.

4 Tungsten and lead calorimeters study at CERN

Since the acceptance of ET6 covers recoil electron energies 6–15 GeV (Fig.2) the tungsten and lead calorimeters was also studied at CERN where the test beams of electron with energies higher then 6 GeV are available. The measurements were performed at the SPS electron test beam H4 at energies 6-27.5 GeV for the tungsten detector and 6-15 GeV for the lead one. The beam size at the face of detector was about 2x2 cm^2 that was defined by the size of the scintillating counter in the trigger. The beam line is equipped with 4 planes of drift chamber (2 planes for every coordinate) in front of the detector which give the particle impact position with accuracy of $\approx 0.02\ mm$. The calorimeter was situated on the platform which can be moved remotely in both x and y directions with the accuracy of $\approx 0.25\ mm$. In the vertical direction the position of the platform was fixed to have the center of the beam in middle horizontal plane of the detector. In the x direction the platform was moved in a way to illuminate by the beam all cells of the calorimeter in several runs.

In CERN tests all 12 cells of W and Pb detectors were active and PMs FEU-147 were used in the readout. The data acquisition and handling were performed with the CMS DAQ system [10].

4.1 Energy response

The study of energy response includes calibration, spatial uniformity, linearity and energy resolution investigations.

The calibration procedure is similar to that was done at DESY test beam.The responses of all cells have been equalized by tuning the high voltage on PMs with accuracy $\approx 10\%$ before taking data with energy and spatial scan. The relative calibration coefficients have been determined off-line by selecting beam hit area 2x2 mm^2 around center of each cell. The off-line fine tuning of geometry yielded in final precision of about 0.1 mm.

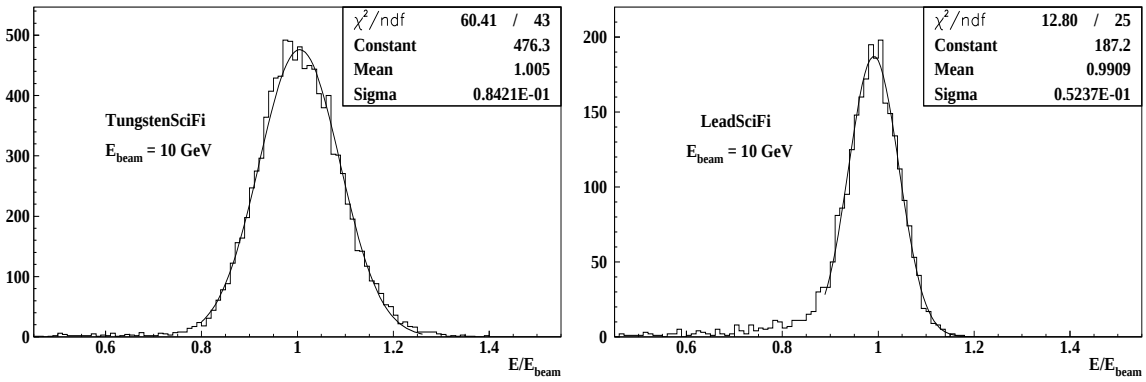

Fig. 12: The normalized energy spectra for tungsten (left) and lead (right) calorimeters at E=10 GeV

To determine linearity and energy resolution the hit points of beam are selected in rectangular area 4(vert.)x12(horiz.) mm^2 around the center of detector. The spectra of energy deposited in calorimeters normalized on the incident beam energy at 10 GeV are shown in Fig.12. They exhibit the gaussian peak and low energy tail originating from the energy leak out of detector. The tail is more pronounced for lead calorimeter because with the same transverse dimensions it

has lower shower containment comparing with tungsten calorimeter. Both calorimeters show linear responses, within 0.5% for tungsten and 1% for lead detector as it follows from the shaded area on Fig.13.

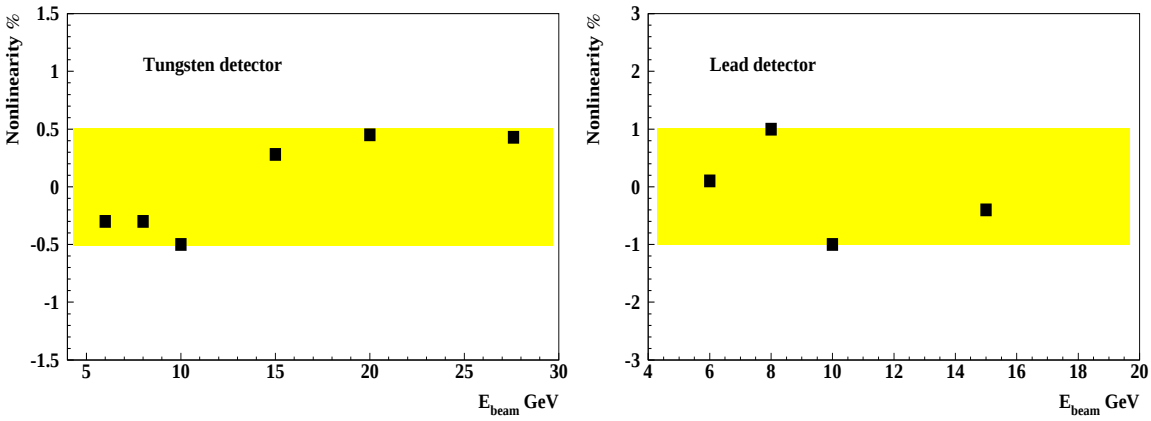

Fig. 13: The response nonlinearity for tungsten (left) and lead (right) calorimeters (errors are included in the marker size).

The dependence of resolution σ_E/E on energy (both DESY and CERN data) is shown on Fig.14 fitted by quadratic sum (3) with stochastic term of $(22.8 \pm 0.4)\%$ for tungsten and $(17.3 \pm\ 0.4)\%$ for lead calorimeter. Constant terms are $(4.16 \pm 0.2)\%$ and $(0.6 \pm\ 0.8)\%$ respectively.

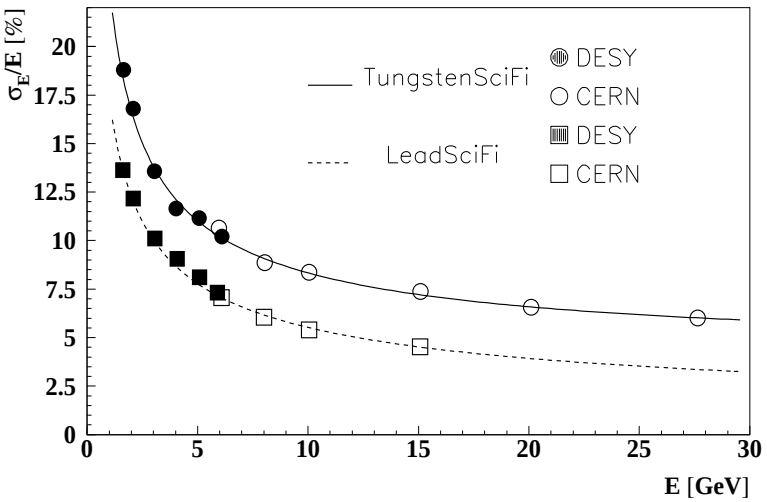

Fig. 14: Energy resolution *vs* beam energy.

The fit of only CERN data gives the following values for stochastic

and constant terms:

$$a = (23.5 \pm 0.6)\%, \quad b = (4.0 \pm 0.2)\% \tag{6}$$

for the tungsten calorimeter. For the lead calorimeter they are

$$a = (16.7 \pm 0.5)\%, \quad b = (1.5 \pm 0.5)\% \tag{7}$$

Comparison with DESY data (see Table 2 for PM FEU-147) shows that DESY and CERN data are compatible for both types of calorimeters.

The experimental values of stochastic terms differ from MC that is mainly due to the photostatistic contribution. The main contribution to constant terms are imperfections in calibration and detector inhomogeneities (especially for tungsten calorimeter).

Uniformity of response was investigated along both horizontal (x) and vertical (y) directions. It is important especially in vertical plane since both detectors have vertical size $\approx 24\ mm$ due to the limited space inside magnet. This size corresponds to about 2.4 Moliere radius for tungsten calorimeter and about 1 Moliere radius for lead detector. The response is uniform within 2.5% for tungsten and within 2% for lead detector (border cells excluded) along x axis. The worse uniformity of tungsten detector can be explained by the fact that with the same geometrical accuracy of space granularity the uniformity of the sampling ratio is worse for the tungsten as compare with the lead detector. On the other hand it is harder technologically to keep geometrical accuracy for tungsten block.

According to MC (Fig.2a) about 99% of the recoil electrons populate area $\pm 4\ mm$ around horizontal beam plane (or middle horizontal plane of detector). Taking into account possible vertical tilt of the e-beam and misalignment of detector we have considered area $\pm 5\ mm$. The behavior of response along y axis for tungsten and lead calorimeter is shown on Fig.15. It can be seen that tungsten detector has more flat behavior of response around middle plane.

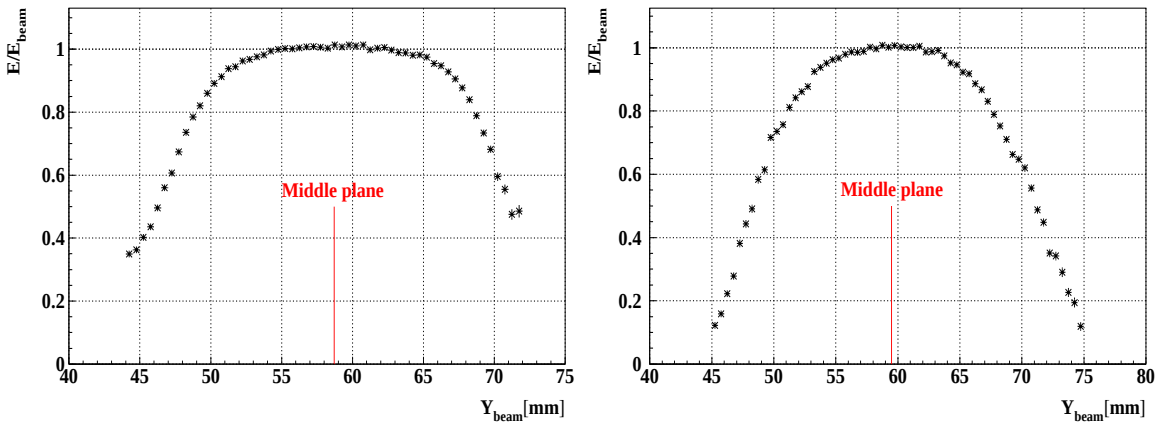

Fig. 15: The response uniformity for W (left) and Pb (right) calorimeters along vertical axis y.

The response is uniform within 2% in the area $\pm 5\ mm$ for tungsten calorimeter as compared with to 4% for lead one.

The behavior of response has been investigated in the region of crack between two blocks of tungsten detector. No significant deviation in response uniformity was found in that region. The channeling effect [11] has been studied for both detectors at incident angles above 2^o (minimal incident angle according to Fig.1) and found to be insignificant.

4.2 Shower profile and space resolution

The shower profile has been measured along x direction of detectors for different energies of the beam, using the coordinate information from drift chambers. The size of the beam in the vertical direction was selected $\pm 2\ mm$ around the middle horizontal plane of detectors. The normalized energy sums of 2x2 adjacent cells on the right (E_R/E_0) and left (E_L/E_0) sides of detector center were plotted as a functions of x coordinate of hitting electron. Fig.16 shows the x-projections of shower profile for both detectors at energy of 10 GeV of incident electron. Data are fitted by sum of two error functions and therefore projection of shower profile on one coordinate can be described by sum of 2 Gaussians as it is shown in Fig.16. The

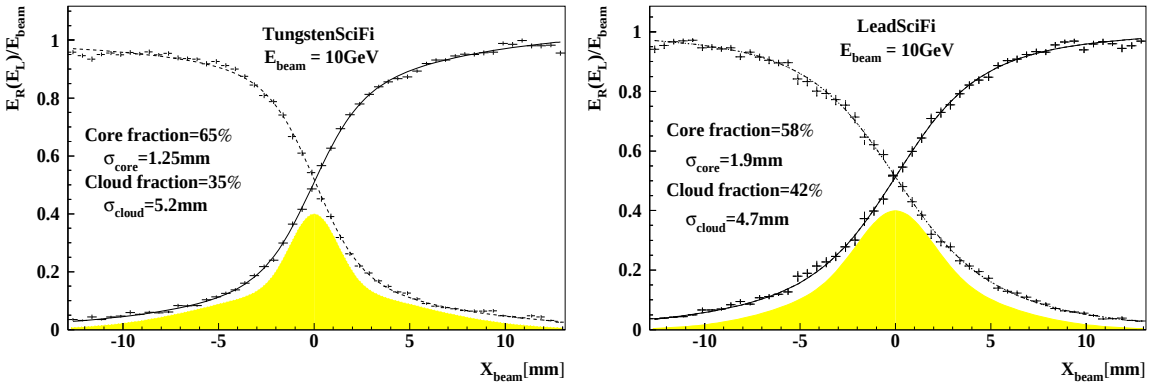

Fig. 16: The shower profile along x-axis in tungsten (left) and lead (right) calorimeters for 10 GeV electrons.

behavior shower profile has been studied at different energies in the range of 6–15 GeV for lead and 6–27.6 GeV for tungsten detector. The shower profile for lead detector is well described with one Gaussian at energies 6 and 8 GeV and with 2 Gaussians at energies 10 and 15 GeV but effective width remains a constant within experimental errors for this energy range ($\sigma_{eff} = (3.4 \pm 0.3)\ mm$). For the tungsten detector the parameters of narrow(core) and wide(cloud) components of the shower remain a constants within experimental errors in the energy region of 6–27.6 GeV and have mean values of $\sigma_{core} = 1.25\ mm$, core fraction=65%, $\sigma_{cloud} = 5.2\ mm$, cloud fraction=35%.

The reconstruction of electron entry point is performed using experimental relative shower sharing function

$$F_{rs} = (A_1 - A_2)/(A_1 + A_2) \tag{8}$$

to take into account shower profile; here A_1, A_2 – energies deposited in adjacent cells(layers) one of which is a cell(layer) with maximum signal or A_1, A_2 are the energies deposited in the cells adjoining a cell with maximum response. The experimental function F_{rs} for two adjacent (upper and lower) horizontal layers of tungsten calorimeter is shown in Fig.17(left), $y_{beam} = 0$ corresponds to borderline between upper and lower layers. The difference of reconstructed (measured) and given by drift chambers (beam) y-coordinates is shown

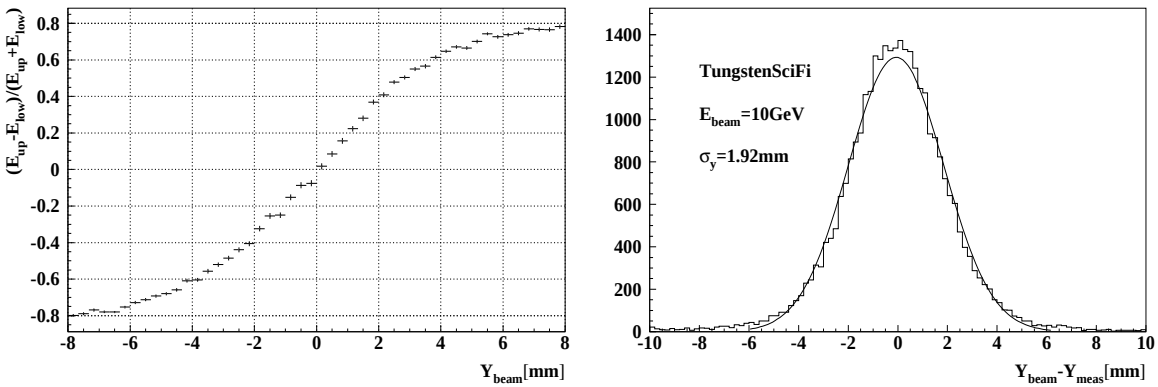

Fig. 17: The experimental relative shower sharing function for tungsten calorimeter (left) and corresponding y-coordinate resolution for 10 GeV electrons (right).

on Fig.17(right) for energy of incident beam 10 GeV. The recon-

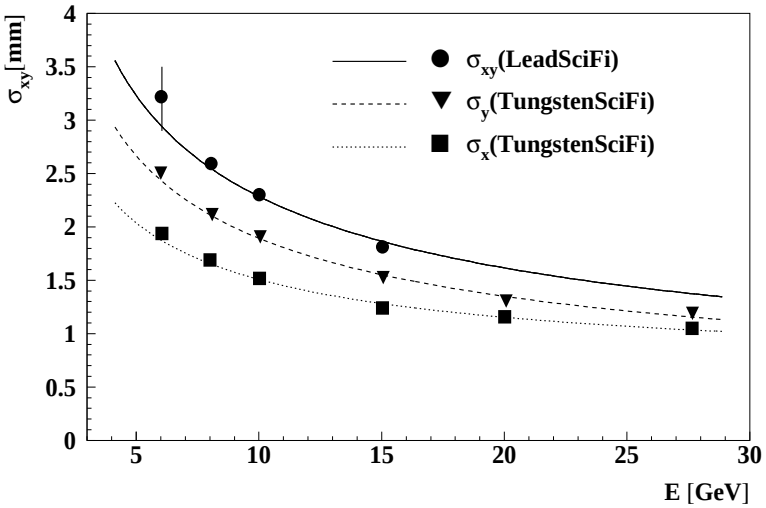

Fig. 18: Coordinate resolution vs beam energy.

struction of x-coordinate of incident electron using in function F_{rs} energies deposited in the cells adjoining cell with maximum response gives some better coordinate resolution in case of tungsten detector. For the lead calorimeter no significant difference is found in choosing function F_{rs} for coordinate reconstruction and coordinate resolutions for x and y directions are approximately the same. The energy dependences of coordinate resolutions for both detectors are shown in Fig.18 together with the data fit by quadratic sum

$$\sigma_{x,y} = c/\sqrt{E} \oplus d \tag{9}$$

The results of the fit can be written as

$\sigma_x = (4.3/\sqrt{E[GeV]} \oplus 0.6)\ mm,\ \sigma_y = (5.9/\sqrt{E[GeV]} \oplus 0.3)\ mm$ $for\ W\ detector$
and
$\sigma_x = \sigma_y = 7.2\ mm/\sqrt{E[GeV]} \quad for\ Pb\ detector.$
As it was expected the measured space resolution is worse than prediction of MC (4,5) which does take into account only shower development fluctuation in calorimeters but not the influence of apparatus effects (PM, cables, noise, etc).

5 Summary and conclusion

In accordance with the proposal [4] on the H1 Luminosity System Upgrade 2000, the SPACAL type small size electron calorimeters for new H1 electron tagger ET6 were constructed in different modifications: tungsten/fibers, lead/fibers, different PMs, *etc.*

The MC simulation for calorimeters were performed and the detectors were studied in the DESY electron test beam at energies 1.6-6 GeV and in the CERN electron test beam at higher energies 6-27.6 GeV. Results of the DESY and CERN beam tests are compatible. There is a reasonable agreement of data on energy resolution with the relevant MC calculations.

Linearity of the calorimeters response is better than 1% which ensures the satisfactory use of these small size calorimeters for electron tagging in the energy region of interest for the H1.

Channeling effects were found to be not essential for the real experiments at the collider HERA since the recoil electrons will hit the calorimeter at the angles larger than 2^o to the fibers.

Consideration of all the data on the energy resolution σ_E/E shows that the best results are achieved for the lead calorimeter with the use of Philips MPs in the readout. On the other hand, some better space resolution $\sigma_{x,y}$ was achieved for the tungsten calorimeter rather

than for the lead one. This is seen from comparison of data for the tungsten detector

$$\sigma_E/E = (18.6/\sqrt{E[GeV]} \oplus 3.2)\%,$$
$$\sigma_x = (4.3/\sqrt{E[GeV]} \oplus 0.6)\ mm,\ \sigma_y = (5.9/\sqrt{E[GeV]} \oplus 0.3)\ mm$$

with the results for the lead one

$$\sigma_E/E = 13.0/\sqrt{E[GeV]}\%,\ \sigma_x = \sigma_y = 7.2/\sqrt{E[GeV]}\ mm.$$

The better energy resolution of lead calorimeter is due to the larger volume ratio of active to passive matter in comparison with the tungsten calorimeter. The last one has the better space resolution because of smaller radiation length.

The overall conclusion of these studies is that the MC simulation and the beam tests have shown that the compact SPACAL type electron detector satisfies the requirements to the tagger ET6 which is used after modification of HERA *ep* collider for tagging the photoproduction events in the frames of H1 upgraded detector, and for measuring the HERA2 Luminosity in conjunction with the photon detector.

Acknowledgments

The authors are thankful to DESY2 and SPS teams who provide the good quality test beams.

References

[1] R.Bacher et al., HERA Luminosity Upgrade (Revised 3rd Draft 30.03.98), http://pia.desy.de:8135/TWDM/cgi/twdmproto.pm

[2] I.Abt et al., NIM A321 (1997) 310.

[3] S.Levonian, H1LUMI - A Fast Simulation Package for the H1 Luminosity System. H1-note H1-04/93-287

[4] V.Andreev et al., Proposal for an Upgrade of the H1 Luminosity System and its Associated Electronics for HERA 2000. DESY PRC-98/05, H1-note H1-06/98-544.

[5] P.S.Baranov et.al., Radiative resistance of material used in scintillation and c'erenkov counters. LPI Preprint 53, 1996

[6] CMS, The Hadron Calorimeter Project, CERN/LHC 97-31, CMS TDR2, 20 June 1997, p.24

[7] T.Nicholls et al., Performance of an Electromagnetic Lead/Scintillating-Fibre Calorimeter. NIM A374 (1996) 149.

[8] T.Nickolls et al., The H1 Lead/Scintillating-Fibre Calorimeter. NIM A386 (1997) 397.

[9] F.Moreau, The communication at the H1 LUMI meeting.

[10] The Electromagnetic Calorimeter Project, CMS TDR 4, CERN/LHCC 97-33, 1997.

[11] Scintillating-Fibre Calorimetry, CERN 95-02, 28 February 1995.